UDC 004.021

Application of filtering efficiency prediction to hyperspectral data pre-processing

V. V. Lukin [1] *, S. S. Krivenko [1], O. S. Rubel [1], S. K. Abramov [1], M. S. Zriakhov [1], M. L. Uss [1], B. Vozel [2], K. Chehdi [2]

[1] *National Aerospace University, Kharkov, Ukraine*

[2] *University of Rennes 1, Lannion, France*

Several approaches to prediction image denoising efficiency for DCT-based filter have been proposed recently. They allow predicting improvement of PSNR (IPSNR) and visual quality metrics as PSNR-HVS-M (IPHVS) for denoised images under condition of noise characteristics known or pre-estimated in advance. Here we apply the prediction approach to pre-processing ten sub-bands of Hyperion hyperspectral data. It is shown that there are sub-band images for which there is no necessity to carry out filtering. Meanwhile, there are sub-bands for which IPSNR reaches 5...9 dB and the use of denoising is expedient.

Keywords: remote sensing, DCT-based filter, efficiency prediction, hyperspectral data

Introduction

Airborne and spaceborne remote sensing (RS) systems are widely used for various applications nowadays [22]. Hyperspectral imagers are a relatively new tool of remote sensing [1, 3]. They potentially provide useful data for extractring different types of information on sensed terrains. However, there are, at least, two obstacles that complicate processing of hyperspectral images with the goals of classification, object detections and others. These obstacles are huge amount of data to be processed due to high resolution of modern hyperspectral systems and hundreds of used sub-bands [4] and noise present acquired images [1, 3, 23]. Therefore, it is desired to carry out image pre-processing (noise removal), at least, for those bands where noise intensity is high enough to sufficiently influence (in negative sense) solving the final tasks of hyperspectral data processing.

Note that there is no need to perform denoising for all sub-bands. There could be different reasons to avoid (skip) denoising. Firstly, noise intensity (or, more strictly, input PSNR) can be such that filtering practically does not remove noise [5, 6]. Secondly, image structure can be such (for example, highly textural) that denoising does not produce positive effect [5, 6, 12, 15, 23]. Then, it is expedient to have some rules and/or means to undertake a decision is it worth filtering a given sub-band image or no. Obviously, such a decision should be fast enough and reliable enough [3]. Meanwhile, it should take into account image properties (complexity) and noise properties (type, intensity, etc.).

There are certain pre-requisites for undertaking such decisions in automatic manner. Firstly, quite accurate methods for blind estimation of noise characteristics (including the cases of signal-dependent noise typical for hyperspectral images [1]) have been designed recently [24, 25]. Their application to real-life hyperspectral acquired images by moderm sensors has confirmed one more time [1, 24, 25] that signal-dependent noise component is usually dominant. Secondly, it has been shown that filtering efficiency for, at least, DCT-based filters [7, 8... +10, 11] can be predicted under condition of accurately estimated noise parameters [16–21] for such parameters characterizing filtering efficiency as improvement of peak signal-to-noise ratio (IPSNR) or improvement of visual quality metric PSNR-HVS-M [14] (IPHVS). To undertake a decision on using or avoiding filtering, these metrics can be used jointly or separately

The goal of this paper is to apply the designed prediction methodology to real life data and to analyze the obtained results from practical viewpoint. For this purpose, we use a group of sub-bands of two Hyperion sensor hyperspectral images.

The paper structure is the following. Section 2 describes the conventional DCT-based filter and the designed methodologies of filtering efficiency prediction. Section 3 presents data on noise properties in hyperspectral data and the results of prediction method application to them. Finally, the conclusions and practical recommendations are presented and discussed.

DCT-based filtering for different noise types and methodologies of prediction

First of all, let us explain why below the DCT-based filtering is considered. One useful property is that it has low computational complexity [11, 15] — this is important since there are many sub-band images that have to be processed and it is possible [3] that this has to be done on-board where computational resources are limited. Another advantage is that, as it has been demonstrated in [12, 15], the DCT-based filter possesses denoising efficiency close to the best known filters (e.g. BM3D [10])

* e-mail: lukin@ai.kharkov.com

Online ISSN 2313-2132

and to potential denoising bounds [4] for images corrupted by additive white Gaussian noise (AWGN):

$$I_{an}^{add}(i,j)=I_t(i,j)+N_G(\sigma), \quad (1)$$

where I_t denotes true image, I_{an}^{add} is noisy image, i and j are image pixel indices, N_G denotes zero mean AWGN with standard deviation of the noise σ.

Recall that DCT-based filtering relates to orthogonal transform based denoising techniques. In the case of AWGN, after direct 2D DCT in each block, the thresholding operation is performed as:

$$\mathrm{B}_{out}^{add}(l,m)=\begin{cases} B_{in}^{add}(l,m) \leftarrow B_{in}^{add}(l,m) > \beta\sigma, \\ 0 \leftarrow B_{in}^{add}(l,m) \le \beta\sigma, \end{cases} \quad (2)$$

where β is a thresholding parameter (the recommended value of which is equal to 2.7), l and m denote spatial frequency indices in an image 8×8 pixels block, B_{in}^{add} denote DCT coefficients of noisy image block, B_{out}^{add} are DCT coefficients after thresholding. After hard thresholding (2), inverse 2D DCT is applied to B_{out}^{add}. The most efficient (standard) DCT-based filter [12] works with full-overlapping of blocks where, at the final stage, data from overlapping blocks are collected for averaging the filtered values for a given pixel.

One more advantage of the DCT-based filtering is that it is applicable to different types of noise. If one deals with signal-dependent noise, the image-noise model is the following [13]:

$$I_{sdn}(i,j)=I_t(i,j)+N(i,j,I_t), \quad (3)$$

where $N(i, j, I_t)$ denotes signal-dependent noise that has zero mean but its probability density function and variance $\sigma^2(i,j,I_t)$, in general, depend upon I_t for a given pixel. We assume that $\sigma^2(i,j,I_t)$ is a priori known or accurately pre-estimated.

Then for signal-dependent spatially uncorrelated noise the thresholding is modified as [13]:

$$\mathrm{B}_{out}^{sd}(l,m)=\begin{cases} B_{in}^{sd}(l,m) \leftarrow B_{in}^{sd}(l,m) > \beta\sigma(l,m), \\ 0 \leftarrow B_{in}^{mult}(l,m) \le \beta\sigma(l,m), \end{cases} \quad (4)$$

where $\beta\sigma(l,m)$ denotes the estimate of local standard deviation of the signal-dependent noise. Note that since I_t in the dependence $\beta\sigma(l,m)$ is different for different pixels of a given block and is unknown for noisy data at hand, it is usually replaced by block mean (can be also replaced by block median).

All other operations including direct and inverse 2D DCT and final averaging of filtered values are the same as for the case of AWGN described above. The DCT-based filtering itself [13] and combined with other techniques [8] is one of the best denoising technique for signal-dependent noise case.

Let us recall a general principle of filtering efficiency prediction. An idea consists in the following. There is some input parameter that is easily computed and that is able to characterize image complexity and noise intensity simultaneously. There is also some output parameter (metric) able to adequately characterize denoising efficiency. These two parameters are strictly connected between each other and this connection is described by an analytical dependence which is known to the moment prediction is needed. In other words, the dependence is obtained off-line (in advance). Then, prediction is carried out as follows. An input parameter is calculated, its value is inserted into the dependence as its argument and the output parameter is calculated. Then this put parameter (predicted value) is used for deciding is it worth filtering or not or for some other purpose (e.g., for setting the filter parameters).

Then, the main goal of preparatory work is to obtain an analytically described dependence of an output parameter on an input parameter. The output parameter could be, e.g., IPSNR (i.e., the difference between the output and input PSNR, expressed in dB) and the input parameter could be, e.g., the probability $\mathrm{P}_{2\sigma}$ [16, 18–21]. This is mean probability that absolute values of DCT coefficients do not exceed $2\beta\sigma(l,m)$ in the considered blocks.

The aforementioned analytical dependence can be obtained in different ways. The simplest one is to use scatter-plots and curve fitting into them. For the scatter-plot points, their arguments are the values of input parameter and vertical axis corresponds to output values. Each scatter-plot point corresponds to one test image with one set of signal dependent noise parameters. The test image is artificially noised with determining input value of a considered metric (e.g., PSNR) and then filtered with determining output value (e.g., output PSNR and, then, IPSNR). We do not go deeply into the questions of how to select test images, what should be sets of parameters of signal-dependent noise, etc. Some details are presented in papers [16, 18–21]. We would like to mention only the following. The number of test images should be large enough (more than ten, desirably about 30...40) and their complexity has to be very different. The cases of prevailing signal-independent and signal-dependent components should be considered and noise intensity has to vary in wide limits. Then, the scatter-plot looks as shown in Fig. 1 and it is possible to fit a curve into it and to analyze accuracy of such fitting. The fitting quality (and, respectively, quality of prediction) can be characterized by different statistical criteria [2]. The most popular of them is goodness of fit (R^2) that should be as close to unity as possible and root mean square error (RMSE) that should be as close to zero as possible.

It is clear that different quality criteria can be predicted with different accuracy. For example, IPSNR is usually predicted more accurately than IPHVS (the latter is also expressed in dB). Prediction also depends upon input parameter, output parameter, used function

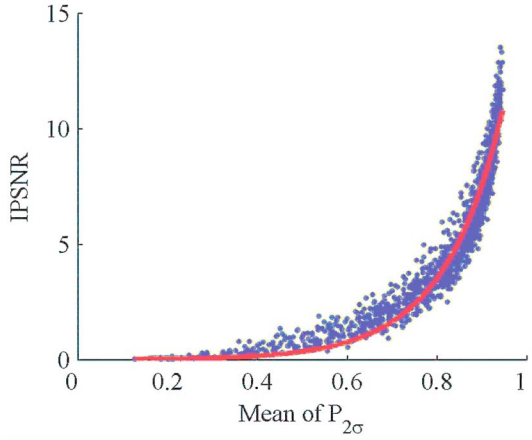

Fig. 1. 1D catterplots of IPSNR for the DCT-based denoising vs mean of local estimates of $P_{0.5\sigma}$

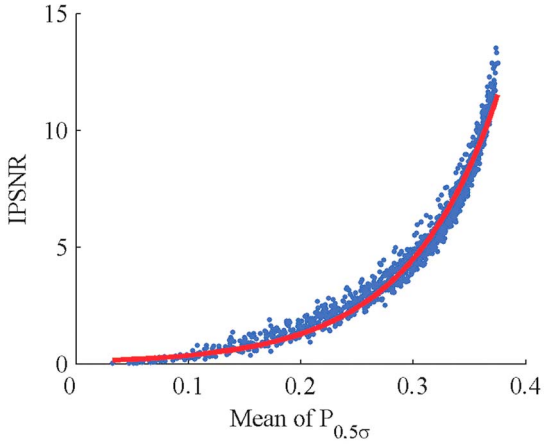

Fig. 2. 1D catterplots of IPSNR for the DCT-based denoising vs mean of local estimates of $P_{0.5\sigma}$

(power, exponential, polynomial) and the number of its free parameters. There are also ways to improve prediction using two or more input parameters [20, 21] and/or optimizing them. However, even for the simplest prediction method (based on a curve fitted into a 1D scatter-plot as in Fig. 1) IPSNR can be predicted with R^2 about 0.95 and RMSE about 0.6...1.0 [20]. This can be acceptable for practical applications.

It is also important that it is enough to estimate $P_{2\sigma}$ locally in non-overlapping or randomly chosen blocks and/or to employ, at least, 300...500 blocks. Due to this, prediction is by about two orders faster than the standard DCT based denoising that, recall, employs two DCTs (direct and inverse) in fully overlapping blocks [11].

If there is only one input parameter, then it is reasonable to apply the probability $P_{0.5\sigma}$ that absolute values of DCT coefficients do not exceed $0.5\sigma(l,m)$ [20]. The scatter-plot is presented in Fig. 2. Analysis of both scatter-plots and fitted curves shows that there are strict monotonous dependences between output and input parameters that allow undertaking decisions based on predicted data. Suppose that IPSNR should be larger than 1 dB to consider filtering useful. Then, roughly saying, it is possible to skip filtering if $P_{2\sigma}$ is less than 0.6 or $P_{0.5\sigma}$ is less than 0.2.

In both cases (Figures 1 and 2), as prediction model, the exponent fitting function was found as the most suitable:

$$Metric_{pred} = a\exp\left(b\overline{P}_{a\sigma}\right), \qquad (5)$$

where $Metric_{pred}$ is a predicted value of a considered metric of denoising efficiency, a and b are coefficients of fitting function, a = 0.5 or 2.0. In particular, for the fitted curve in Fig. 1, a = 0.00797 and b = 7.62 whilst for the curve in Fig. 2 the parameters are a = 0.11 and b = 12.53. Similarly, IPHVS can be predicted but with less accuracy (larger RMSE and smaller R2 [20, 21]). Thus, we have methodology of prediction and the task now is to verify it for real life data.

Application of Prediction to Real-Life Data

First of all, it is needed to have some imagination on properties of noise in hyperspectral images. For the model (3), one has for n-th sub-band

$$\sigma^2_{ij}(n) = \sigma^2_0(n) + k(n)I_t(i,j,n), \qquad (6)$$

where $\sigma^2_0(n)$ denotes the signal-independent (SI) noise variance and $k(n)$ is the signal-dependent (SD) noise parameter. Both parameters $\sigma^2_0(n)$ and $k(n)$ are often assumed to be non-negative. This assumption is based on physical properties and it can be used as certain restrictions in methods of noise parameters estimation (negative estimates of the considered parameters can be assigned zero values).

Fig. 3 presents the estimates of these parameters obtained by the method [24] for datasets of Hyperion data (taken from http://eros.usgs.gov/). There are two groups of sub-bands with indices 1...12, 62...77 and 231...240 that are not used in analysis due to very bad quality of images in them. Because of this, noise parameter estimates for them are not presented in plots.

Estimate analysis shows the following. First, for all three datasets the estimates' dependences on sub-band index behave similarly. Second, there is more intensive noise (both larger estimates of $\sigma^2_0(n)$ and $k(n)$ for images at the edges of sensor ranges, e.g., for sub-bands with indices 13...15 and 59...61. Noise is seen well for visualized images for these sub-bands. Meanwhile, the noise is one-two order less intensive in the middle of this range. In fact, noise is of such intensity (more exactly, PSNR is as high) that noise is practically not seen in visualized sub-band images with indices about 35...40. Third, it is possible to evaluate contribution of SD noise component by calculating equivalent noise variance for it as

$$\widehat{\sigma}^2_{eqSD}(n) = \sum_{i=1}^{I_{\text{Im}}}\sum_{j=1}^{J_{\text{Im}}} k(n)I_t(i,j,n)/(I_{\text{Im}}J_{\text{Im}}) \approx$$
$$\approx \sum_{i=1}^{I_{\text{Im}}}\sum_{j=1}^{J_{\text{Im}}} \hat{k}(n)I^n(i,j,n)/(I_{\text{Im}}J_{\text{Im}}) = \hat{k}(n)I_{mean}(n) \qquad (7)$$

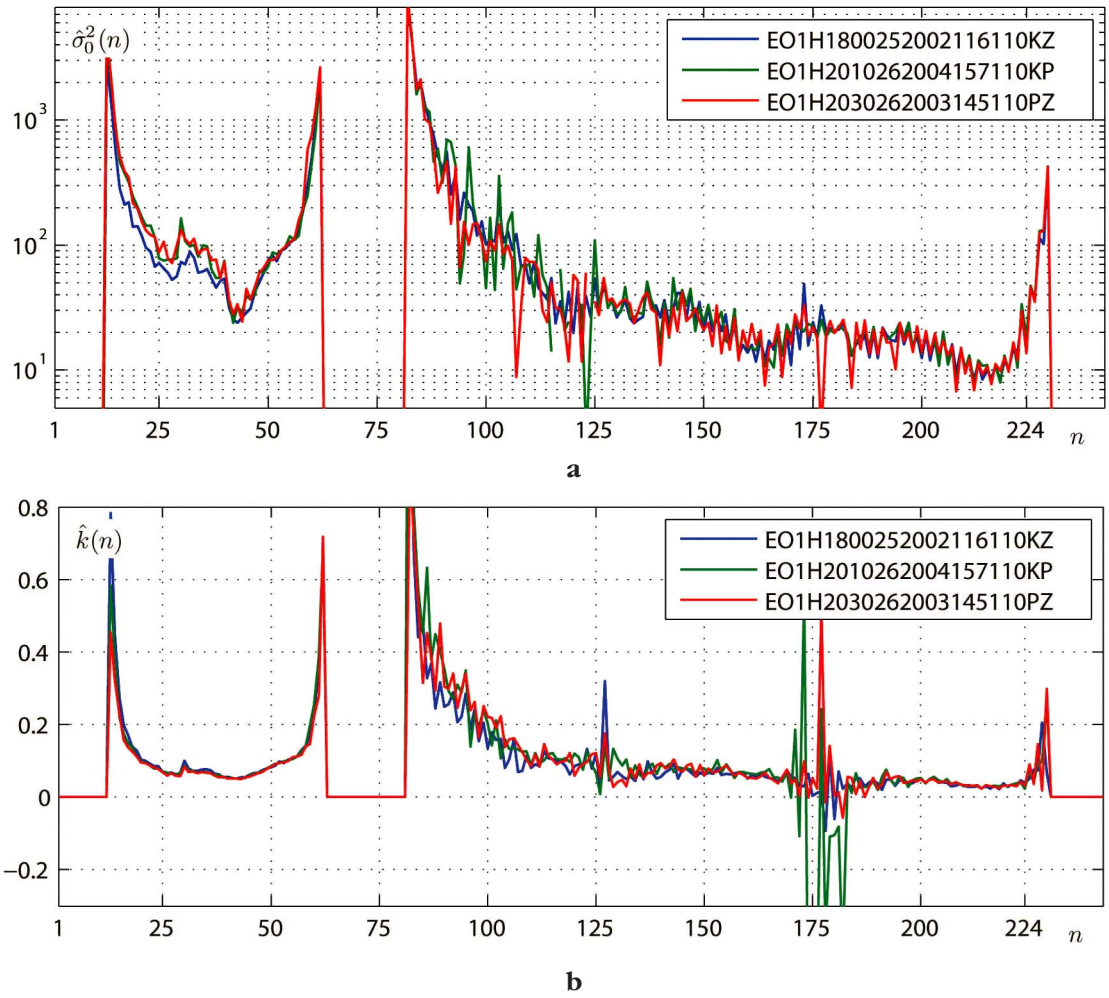

Fig. 3. The estimates $\sigma_0^2(n)$ and k (n) for sub-bands of three sets of Hyperion data

where $I_{mean}(n)$ defines image mean for an n-th sub-band. Then this equivalent variance can be compared to $\sigma_0^2(n)$. Such comparisons were performed in [25] and it has been shown that for most sub-bands $\tilde{\sigma}_{eg\,SD}^2(n)$ is of the same order as $\sigma_0^2(n)$ or larger. This means that SD character of the noise should be taken into consideration in processing and analysis of hyperspectral data. The exceptions could be several sub-bands (see the plots in Fig. 3) where the estimates $k(n)$ are negative This mostly happens due to imperfectness of the estimation method and for sub-bands with very high PSNR.

Having the estimates of signal-dependent noise parameters and assuming their high accuracy, it becomes possible to predict filtering efficiency. Since we do not have noise-free images, it is impossible to evaluate how accurate prediction is. But it is possible to compare the prediction results for different input parameters and to analyze the observed tendencies.

In our analysis, we have considered the sub-bands with indices 13...22. As it follows from analysis of the plots in Fig. 3, there is a tendency to noise intensity reduction for them. This tendency is supported by numerical data presented in Tables 1 and 2. Meanwhile, dynamic range for these images remains practically the same. Thus, there is the tendency to increasing of input PSNR. Du to this, the largest values of $P_{2\sigma}$ are observed for the 13-th sub-band (recall that $P_{2\sigma}$ is large (approaches to the maximally possible value of 0.95) for simple structure images and high intensity noise.

According to prediction dependence (fitted approximating curve) in Fig. 1, IPSNR and IPSNR-HVS-M increase if $P_{2\sigma}$ is larger. Because of this, the maximal expected positive effect of filtering is predicted for 13-th sub-band image. This effect is quite large – predicted IPSNR (based on $P_{2\sigma}$) reaches 5.6 dB for the first dataset and 9.06 dB for the second dataset. Such improvement should be obviously seen if input and output images are compared visually. This is possible to do. Fig. 4 presents original (noisy) and output (filtered) images in 13-th sub-band of the dataset EO1H1800252002116110KZ. Whilst noise is visible in original image (especially in homogeneous image regions), it is effectively suppressed in output image alongside with good preservation of important details and edges.

Meanwhile, there are also many sub-bands for which IPSNR predicted on basis of $P_{2\sigma}$ is of the order of 1 dB or less. Simultaneously, predicted values of IPHVS (see data in the rightmost columns in Tables 1 and 2) are even

Table 1.
Noise parameters and prediction results for sub-band images with indices 13...22 of Hyperion sensor dataset EO1H2010262004157110KP

Subband Index n	$\sigma(n)$	$k(n)$	Dynamic range	$P_{2\sigma}$	Predicted IPSNR based on $P_{2\sigma}$	Predicted IPSNR based on $P_{2.7\sigma}$	Pred. IPSNR based on $P_{0.5\sigma}$	Pred. IPHVS based on $P_{2\sigma}$
13	63.61	0.78	4166.00	0.85	5.60	4.72	5.90	3.45
14	41.54	0.62	4098.00	0.78	3.84	3.31	4.09	2.19
15	27.38	0.49	4316.00	0.71	2.42	2.08	2.65	1.25
16	20.01	0.42	4411.00	0.64	1.70	1.44	1.92	0.82
17	17.45	0.39	4418.00	0.63	1.56	1.32	1.77	0.74
18	16.64	0.37	4615.00	0.62	1.44	1.23	1.64	0.67
19	14.09	0.34	4741.00	0.59	1.27	1.07	1.47	0.57
20	13.29	0.31	4885.00	0.57	1.10	0.91	1.30	0.48
21	12.05	0.31	5007.00	0.54	0.96	0.78	1.15	0.41
22	10.98	0.30	4872.00	0.52	0.83	0.65	1.00	0.34

Table 2.
Noise parameters and prediction results for sub-band images with indices 13...22 of Hyperion sensor dataset EO1H1800252002116110KZ

Subband Index n	$\sigma(n)$	$k(n)$	Dynamic range	$P_{2\sigma}$	Predicted IPSNR based on $P_{2\sigma}$	Predicted IPSNR based on $P_{2.7\sigma}$	Pred. IPSNR based on $P_{0.5\sigma}$	Pred. IPHVS based on $P_{2\sigma}$
13	54.44	0.78	1793.00	0.93	9.06	7.33	9.43	6.17
14	36.39	0.45	1835.00	0.88	6.85	5.80	7.20	4.40
15	23.74	0.27	1894.00	0.81	4.35	3.86	4.68	2.54
16	16.85	0.20	1985.00	0.73	2.80	2.53	3.11	1.49
17	14.48	0.17	1943.00	0.70	2.41	2.16	2.71	1.24
18	14.83	0.14	2118.00	0.67	2.02	1.80	2.30	1.01
19	11.84	0.13	2190.00	0.63	1.58	1.38	1.84	0.75
20	11.91	0.10	2265.00	0.60	1.33	1.13	1.57	0.61
21	10.90	0.10	2321.00	0.58	1.14	0.94	1.35	0.50
22	9.77	0.09	2226.00	0.55	1.00	0.80	1.15	0.43

less than 1 dB. This means that improvements according to the considered metrics due to filtering are negligible.

This is seen well in Fig. 5 where input and output images for 22-th sub-band are represented. Noise in the original image can be hardly noticed and the processed (filtered) image looks practically the same as input one. Thus, there is no need in filtering this image.

Three other observations that follow from analysis of data in Tables 1 and 2 are the following. First, all three predictions (based on $P_{2\sigma}$, $P_{2.7\sigma}$ [16], and $P_{0.5\sigma}$) are quite close. This means that, in fact, all three input parameters can be used in practice. Second, predicted IPHVS are always smaller than IPSNR (both are expressed in dB and, thus, can be compared). This is typical for denoising where IPSNR of about 1...3 dB does not guarantee improvement of visual quality. Third, improvement depends upon image complexity. The considered fragment of the dataset EO1H1800252002116110KZ (Fig. 4) is less complex than the analyzed fragment of the other dataset because there are quite large homogeneous image regions in it. The analyzed fragment for the dataset EO1H2010262004157110KP is represented in Fig. 6 where Fig. 6a shows original image in 13-th sub-band. It has smaller homogeneous regions and more edges and details. Due to this, noise is less visible and can be noticed mainly in lighter color (higher mean intensity) parts of the image.

The filtered image is given in Fig. 6b and it is seen tht noise is suppressed whilst useful information is preseved. Visual analysis of input and output images for oher sub-bands has been carried out as well. Starting fom n about 18 it becomes difficult to find differences. Tis means that, on one hand, filtering does not introuce distortions and this is valuable advantage of the DCT-based filter (e.g., the standard median filter introduces visible distortions in such cases). On the other hand, this means that there is no need to apply filtering and it can be skipped. This can accelerate processing of hyperspectral data where, in fact, filtering can be skipped for about 70...80% of sub-bands. This can be especially important for on-board processing of data.Suppose that the rule for avoiding filtering is the following: skip denoising of a given sub-band image if $P_{2\sigma} > 0.6$ (see Fig. 1). Then, there is no need to perform image filtering for sub-bands with n>18 of the subset EOH2010262004157110KP and n>20 for the subset EO1H1800252002116110KZ (see data in Tables).

Conclusions

The method of denoising efficiency prediction is described and tested for real-life multichannel images corrupted by signal-dependent noise. It is shown that the metrics IPSNR and IPSNR-HVS-M can be predicted rather well.

Online ISSN 2313-2132

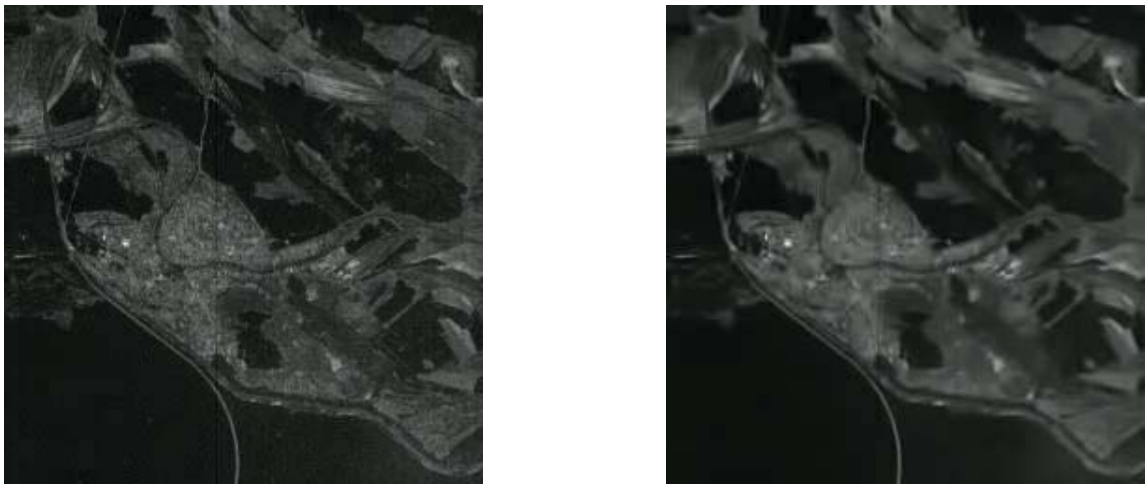

a b

Fig. 4. Input (a) and output (b) images in the 13-th sub-band of Hyperion data

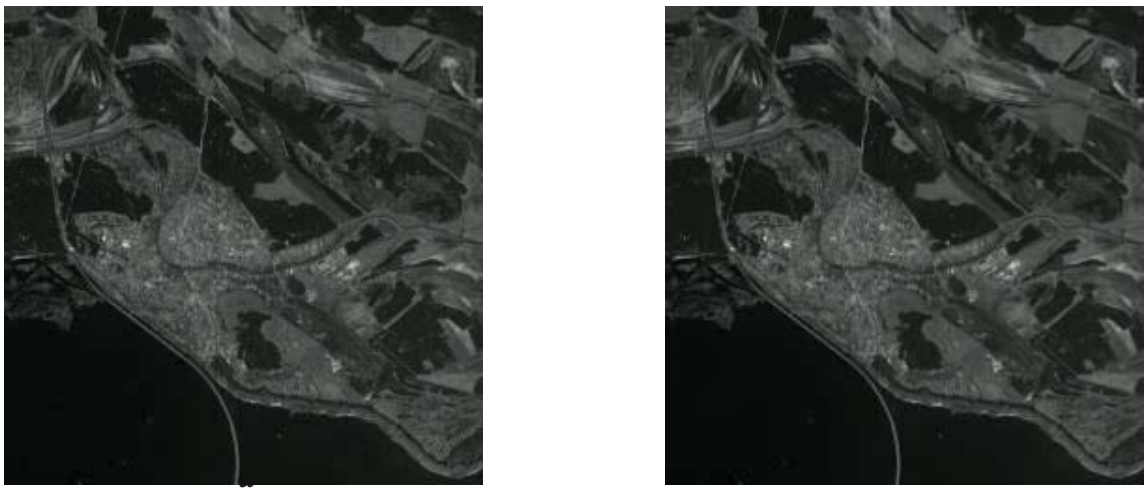

a b

Fig. 5. Input (a) and output (b) images in the 22-th sub-band of Hyperion data

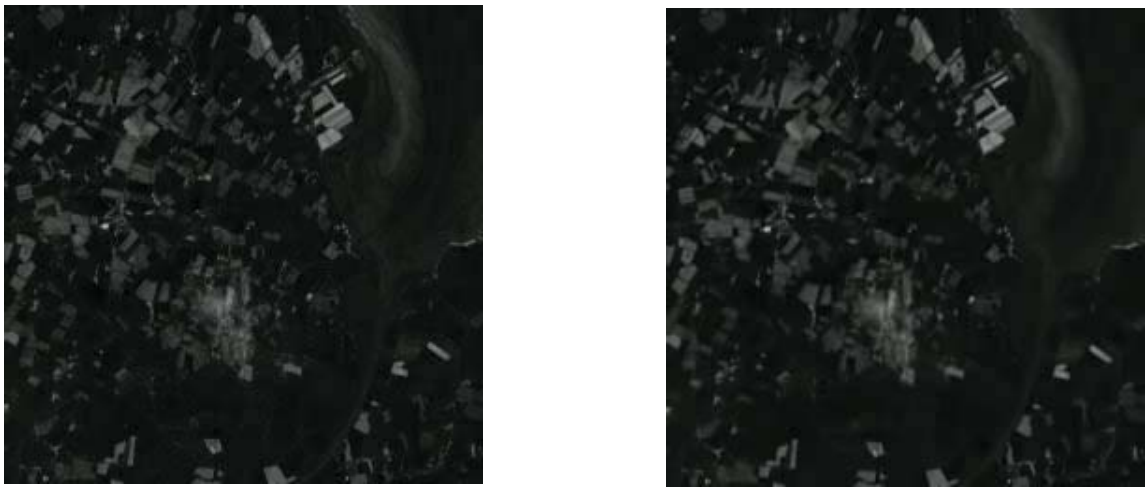

a b

Fig. 6. Input (a) and output (b) images in the 13-th sub-band of Hyperion data

Based on such prediction, it is possible to undertake decisions on applying image denoising to a given sub-band images or skipping this operation if, supposedly, it is practically useless. It is demonstrated that there are quite many sub-band images in hyperspectral data for which the use of denoising is expedient since considerable improvement of image quality can be provided. The corresponding illustrations are given.

References

1. Acito N. Signal-dependent noise modeling and model parameter estimation in hyperspectral images / N. Acito, M. Diani, G. Corsini // IEEE Transactions on Geoscience and Remote Sensing. — 2011. — Vol. 49. — No 8. — P. 2957–2971.
2. An R-squared measure of goodness of fit for some common nonlinear regression models / C. Cameron, A. Windmeijer, A. G. Frank, H. Gramajo, D. E. Cane, C. Khosla // Journal of Econometrics. — 1997. — Vol. 77. — No 2. — P. 329–342.
3. Approaches to Automatic Data Processing in Hyperspectral Remote Sensing / V. Lukin, S. Abramov, N. Ponomarenko, S. Krivenko, M. Uss, B. Vozel, K. Chehdi, K. Egiazarian, J. Astola // Telecommunications and Radio Engineering. — 2014. — Vol. 73. — No 13. P. 1125–1139.
4. Christophe E. Hyperspectral Data Compression Tradeoff / E. Christophe // Optical Remote Sensing. Advances in Signal Processing and Exploitation Techniques, Springer.— 2011. — Vol. 8. — P. 9–29.
5. Chatterjee P. Practical Bounds on Image Denoising: From Estimation to Information / P. Chatterjee, P. Milanfar // IEEE Transactions on Image Processing. — May 2011. — Vol. 20. — No 5. — P. 1221–1233.
6. Chatterjee P. Is Denoising Dead / P. Chatterjee, P. Milanfar / / IEEE Transactions on Image Processing. — 2010. — Vol. 19. — No 4. — P. 895–911.
7. Denoising of single-look SAR images based on variance stabilization and non-local filters / M. Makitalo, A. Foi, D. Fevralev, V. Lukin // Proceedings of MMET. — 2010. — 4 p.
8. Efficiency Analysis of Combined Despeckling of Single-Look SAR Images / R. A. Kozhemiakin, S. S. Krivenko, V. V. Lukin, R. C. P. Marques, F. N. S. de Medeiros, B. Vozel // Aerospace Engineering and Technology. — 2013. — Vol. 5.— No 102. — P. 102–111.
9. Exploiting patch similarity for SAR image processing: the nonlocal paradigm / C.-A. Deledalle, L. Denis, G. Poggi, F. Tupin, L. Verdoliva // IEEE Signal Processing Magazine, Recent Advances in Synthetic Aperture Radar Imaging. — 2014. — 8 p.
10. Image denoising by sparse 3-D transform-domain collaborative filtering / K. Dabov, A. Foi, V. Katkovnik, K. Egiazarian // IEEE Transactions on Image Processing. — 2007. — Vol. 16. — No 8. — P. 2080–2095.
11. Image filtering based on discrete cosine transform / V. Lukin, R. Oktem, N. Ponomarenko, K. Egiazarian // Telecommunications and Radio Engineering. — 2007. — Vol. 66. — No 18. — P. 1685–1701.
12. Image Filtering: Potential Efficiency and Current Problems / V. Lukin, S. Abramov, N. Ponomarenko, K. Egiazarian, J. Astola // Proceedings of ICASSP, Prague. — May 2011. — P. 1433–1436.
13. Local Transform-based Denoising for Radar Image Processing / Egiazarian K.O., Melnik V.P., Lukin V.V., Astola J.T. // Proceedings of IS&T/SPIE International Conference on Nonlinear Image Processing and Pattern Analysis XII, San Jose, CA, USA. — 2011. — SPIE Vol. 4304.— P. 170–178.
14. On between-coefficient contrast masking of DCT basis functions / N. Ponomarenko, F. Silvestri, K. Egiazarian, M. Carli, J. Astola, V. Lukin // Proceedings of the Third Int. Workshop on Video Processing and Quality Metrics, USA.— 2007. — Vol. 3. — 4 p.
15. Pogrebnyak O. Wiener discrete cosine transform-based image filtering / O. Pogrebnyak, V. Lukin // SPIE: Journal of Electronic Imaging. — 2012. — Vol. 21. — Is. 4. — 15 p.
16. Prediction of DCT-based Denoising Efficiency for Images Corrupted by Signal-Dependent Noise / S. Krivenko, V. Lukin, B. Vozel, K. Chehdi // Proceedings of IEEE 34th International Scientific Conference Electronics and Nanotechnology, Kiev, Ukraine. — 2014. — P. 254–258.
17. Prediction of Filtering Efficiency for DCT-based Image Denoising / S. Abramov, S. Krivenko, A.Roenko, V. Lukin, I. Djurovic, M. Chobanu // Proceedings of MECO, Budva, Montenegro. — 2013. — P. 97–100.
18. Rubel O. S. Prediction of Despeckling Efficiency of DCT-based filters Applied to SAR Images / O. S. Rubel, V. V. Lukin. F.S. de Medeiros // Proceedings of DCOSS, Fortaleza, Brazil. — 2015. — P. 159–168.
19. Rubel A. Efficiency of DCT-based denoising techniques applied to texture images / A. Rubel, V. Lukin, O. Pogrebnyak // Proceedings of MCPR, Cancun, Mexico. — 2014. — P. 261–270.
20. Rubel O. An Improved Prediction of DCT-Based Filters Efficiency Using Regression Analysis / O. Rubel, V. Lukin // Information and Telecommunication Sciences, Kiev, Ukraine. — 2014. — Vol. 5. — No 1. — P. 30–41.
21. Rubel A. A Neural Network Based Predictor of Filtering Efficiency for Image Enhancement / A. Rubel, A. Naumenko, V. Lukin // Proceedings of MRRS, Kiev, Ukraine. — 2014. — P. 14–17.
22. Schowengerdt R. A. Remote Sensing: Models and Methods for Image Processing: Third edition / R. A. Schowengerdt / / Academic Press, San Diego, CA. — 2007. — 515 p.
23. Zhong P. Multiple-Spectral-Band CRFs for Denoising Junk Bands of Hyperspectral Imagery / P. Zhong, R. Wang // IEEE Transactions on Geoscience and Remote Sensing. — 2013. — Vol. 51. — No 4. — P. 2260–2275.
24. Local signal-dependent noise variance estimation from hyperspectral textural images / M. Uss, B. Vozel, V. Lukin, K. Chehdi // IEEE J. Sel. Top. Signal Process. — 2011. — Vol. 5. — No. 3. — P. 469–486.
25. On Noise Properties in Hyperspectral Images / S. Abramov, M. Uss, V. Abramova, V. Lukin, B. Vozel, K. Chehdi // Proceedings of IGARSS, Milan, Italy. — 2015. — 4 p.

Online ISSN 2313-2132

ПРИМЕНЕНИЕ ПРОГНОЗИРОВАНИЯ ЭФФЕКТИВНОСТИ ФИЛЬТРАЦИИ К ОБРАБОТКЕ ГИПЕРСПЕКТРАЛЬНЫХ ДАННЫХ

В. В. Лукин, С. С. Кривенко, А. С. Рубель, С. К. Абрамов, М. С. Зряхов, М. Л. Усс, Б. Возель, К. Шеди

Недавно были предложены несколько подходов к прогнозированию эффективности ДКП-фильтров. Они позволяют прогнозировать повышение ПОСШ (IPSNR) и улучшение метрики визуального качества PSNR-HVS-M (IPHVS) для обработанных изображений при условии, что характеристики помех известны или предварительно оценены. В статье прогнозирование применено к предварительной обработке десяти соседних каналов гиперспектральных данных сенсора Гиперион. Показано, что есть каналы, для которых не имеет смысла применять фильтрацию. Вместе с тем, есть и каналы, для которых IPSNR достигает 5...9 дБ и, соответственно, применение фильтрации целесообразно.

Ключевые слова: дистанционное зондирование, ДКП-фильтр, прогнозирование эффективности, гиперспектральные данные

ЗАСТОСУВАНЯ ПРОГНОЗУВАННЯ ЕФЕКТИВНОСТІ ФІЛЬТРАЦІЇ ДО ОБРОБКИ ГІПЕРСПЕКТРАЛЬНИХ ДАНИХ

В. В. Лукін, С. С. Кривенко, О. С. Рубель, С. К. Абрамов, М. С. Зряхов, М. Л. Усс, Б. Возель, К. Шеді

Нещодавно було запропоновано декілька підходів до прогнозування ефективності ДКП-фільтрів. Вони дозволяють прогнозувати збільшення РВСШ (IPSNR) та покращення метрики візуальної якості PSNR-HVS-M (IPHVS) для оброблених зображень за умови, що характеристики завад є відомим або попередньо оцінені. В статті прогнозування застосовано до попередньої обробки десяти каналів гіперспектральних даних сенсора Гіперіон. Показано, що є канали, для яких немає сенсу застосовувати фільтрацію. Втім, є й канали, для яких IPSNR сягає 5...9 дБ і, відповідно, застосування фільтрації є доцільним.

Ключові слова: дистанційне зондування, ДКП-фільтр, прогнозування ефективності, гіперспектральні дані